

Descent Equation for superloop and cyclicity of OPE

A.V. BELITSKY

*Department of Physics, Arizona State University
Tempe, AZ 85287-1504, USA*

Abstract

We study the so-called Descent, or \bar{Q} , Equation for the null polygonal supersymmetric Wilson loop in the framework of the pentagon operator product expansion. To properly address this problem, one requires to restore the cyclicity of the loop broken by the choice of OPE channels. In the course of the study, we unravel a phenomenon of twist enhancement when passing to a cyclically shifted channel. Currently, we focus on the consistency of the all-order Descent Equation for the particular case relating the NMHV heptagon to MHV hexagon. We find that the equation establishes a relation between contributions of different twists and successfully verify it in perturbation theory making use of available bootstrap predictions for elementary pentagons.

1 Introduction

The superamplitude \mathcal{A}_N in planar $\mathcal{N} = 4$ superYang-Mills theory is known to be dual to the superWilson loop [1, 2, 3, 4, 5, 6]

$$\mathcal{W}_N = \exp \left(ig \oint_{C_N} \mathbb{A} \right), \quad (1)$$

defined by a superconnection \mathbb{A} residing on a piecewise light-like contour C_N in chiral superspace. The \mathcal{W}_N , being an off-shell correlator, provides a fully nonperturbative description of \mathcal{A}_N . What makes this correspondence even more powerful is that \mathcal{W}_N can be systematically analyzed in the multi-collinear regimes, i.e., when certain adjacent links become parallel [7, 8, 9, 10]. This expansion receives a rigorous nonperturbative reincarnation within the so-called pentagon operator product expansion (OPE) [11]. The power of the latter lies in the fact that all of its ingredients can be computed to all orders in 't Hooft coupling making use of the hidden integrability of the theory [11, 12, 13, 14, 15, 16, 17, 20, 21, 22]. In spite of the fact that there is a plethora of data on scattering amplitudes that heavily relies on ordinary and dual superconformal symmetries [23, 24, 25, 26], the above formalism obscures the most basic symmetries such as supersymmetry, cyclicity etc.

The chiral nature of the superWilson loop representation itself, while preserves some tree-level dual symmetries, masks others and makes them coupling dependent in spite of the fact that there are no intrinsic short-distance anomalies associated with them¹. One particular generator that received a close attention in this regard was the Poincaré supersymmetry \bar{Q} [26, 27], i.e., the chiral conjugate of Q . Its action on the superloop was cast in an all-loop conjecture² [26] that was dubbed the Descent Equation, see Eq. (6) below. Its power was uncovered in the fact that it mixes different orders in perturbative series, enabling one to predict higher loop amplitudes from the ones an order lower. Of particular importance for this application was the cyclicity of the loop that provided contributions adding up together to yield correct final answer. As a consequence, the goal of the current study will be twofold. We will unravel how the cyclic contributions are implemented in the Descent Equation from the point of view of OPE. And then we will realize what the Descent Equation imply for the mixing of different twists in the operator series.

Our subsequent presentation is organized as follows. In the following section, we recap the form of the equation for the finite Wilson loop observables which are natural from the point of view of the pentagon OPE. Next, we provide a preliminary discussion of the equation relating one-loop NMHV heptagon to two-loop MHV hexagon at leading twist in flux-tube excitations. As we observe there, to properly incorporate cyclic contributions we have, in principle, to resum the entire OPE series. To start with, we go beyond leading twist and uncover the form of the Wilson loop at twist two in Sections 4.2 and 4.3. To guide ourselves in the quest of uncovering cyclicity, we use available exact one-loop expressions for the heptagon and conjecture the form of cyclic contributions in terms of OPE data. Making use of all-order predictions, we then verify that it is indeed correct by going to one loop order higher when all genuine two-particle states start to contribute. Finally we conclude.

¹Of course, there are generators that do develop true anomalies due to ultraviolet divergencies, like conformal boost etc.

²To date, the Descent Equation viewed as a Ward identity of the antichiral supersymmetry generator has evaded rigorous studies due to lack of a proper regularization scheme that leaves manifest symmetries of the superloop intact. The main culprit in these analyses is the correlation functions of field equations of motion with superholonomies and strong UV divergencies associated with light-cone nature of the contour [6].

2 Collinear limit and Descent Equation

A natural observable from the point of view of OPE is a properly subtracted superWilson loop \mathcal{W}_N . It is related to the ratio function $\mathcal{R}_N = \mathcal{A}_N/A_N^{\text{BDS}}$ that was devised in Ref. [26] according to

$$\mathcal{W}_N = \mathcal{R}_N W_N^{\text{U}(1)}. \quad (2)$$

Here $\ln W_N^{\text{U}(1)}$ is the sum of connected correlators of Wilson loops in U(1) theory between reference squares in a chosen tessellation of the N -gon with the coupling constant $g_{\text{U}(1)}^2$ replaced by (one quarter of) the exact cusp anomalous dimensions in $\mathcal{N} = 4$ theory, $\Gamma(g) = 4g^2 - 8g^4\zeta_2 + \dots$,

$$\ln W_N^{\text{U}(1)} = \frac{1}{4}\Gamma(g)X. \quad (3)$$

The function X depends on $3N - 5$ conformal cross ratios $X = X(u_1, \dots, u_{3N-5})$. The superloop admits a terminating expansion in Grassmann variables,

$$\mathcal{W}_N = \sum_{n=0}^{N-4} \mathcal{W}_{N,n}, \quad (4)$$

with each term being a degree- $4n$ polynomials. They correspond to N^n MHV amplitudes, up to an overall factor of the 't Hooft coupling, namely, $\mathcal{W}_{N,n} = g^{2n} \mathcal{A}_{N,n}$.

The action of the \bar{Q} -operator,

$$\bar{Q}_a^A = \sum_{n=1}^N \chi_n^A \frac{\partial}{\partial Z_n^a}, \quad (5)$$

on the N -point N^n MHV observable can be cast in the form

$$\bar{Q}_\alpha^A \mathcal{W}_{N,n} = \frac{\Gamma(g)}{4g^2} \sum_i^{N+1} \int d^{2|3} \mathcal{Z}_{\alpha i}^A [\mathcal{W}_{N+1,n+1} - \mathcal{W}_{N+1,1}^{\text{tree}} \mathcal{W}_{N,n}], \quad (6)$$

where in the right-hand side one takes a collinear limit of an $N + 1$ point N^{n+1} MHV Wilson loop. Notice an extra factor of $1/g^2$ in the above equation that arises due to the aforementioned conversion from amplitudes to Wilson loops. The limit is accomplished by means of a proper parametrization of the near-collinear expansion of adjacent sites parametrized by supertwistors $\mathcal{Z}_i = (Z_i, \chi_i)$ built from momentum twistors Z_i [28] and their Grassmann counterparts χ_i . A particularly convenient form is gained in the OPE framework by encoding all inequivalent polygons with the action of symmetries of intermediate squares, see Appendix A. For the case at hand, the supersymmetric collinear limit emerges from the relation

$$\mathcal{Z}_1^{(n)} = \mathcal{Z}_n^{(n)} - e^{-\tau'} \mathcal{Z}_{n-1}^{(n)} + e^{-\tau'+2\sigma'} (1 + e^{-\tau'-\sigma'+i\phi'}) \mathcal{Z}_2^{(n)} + e^{-2\tau'+\sigma'+i\phi'} \mathcal{Z}_3^{(n)}, \quad (7)$$

and subsequently taking $\tau' \rightarrow \infty$. This implies an expansion at the bottom of the polygon in terms of flux-tube excitations of increasing twists. The measure $d^{2|3} \mathcal{Z}_1$ [26], however,

$$d^{2|3} \mathcal{Z}_{\alpha 1}^A = \oint_{|\varepsilon|=0_+} \frac{d\varepsilon' \varepsilon'}{2\pi i} \int d\varepsilon^{2\sigma'} \int (d^3 \chi_1)^A \bar{n}_\alpha, \quad (8)$$

— where we defined $\varepsilon' = e^{-\tau'}$ and $\bar{n}_\alpha = \varepsilon_{\alpha\beta\gamma\delta} Z_{n-1}^\beta Z_n^\gamma Z_1^\delta$, — singles out one flux-tube fermion.

3 Preliminaries on Descent Equation

The right-hand side of the Descent Equation projects out a single fermionic excitation on the bottom of the polygon, while the top can absorb any multi-particle states with fermionic quantum numbers. Let us, however, start our analysis by considering its left-hand side. We will focus on the MHV hexagon as a case of study. At leading twist, it receives a contribution from a single gauge field created from the vacuum in the operator channel chosen by the parametrization of the momentum twistors introduced in the Appendix A,

$$\mathcal{W}_{6,0} = 1 + (e^{i\phi} + e^{-i\phi})e^{-\tau}\mathcal{W}_{6[1](2)} + \dots, \quad (9)$$

with³ [16]

$$\mathcal{W}_{6[1](2)} = \int_{\mathbb{R}} d\mu_{\mathbf{g}}(v). \quad (10)$$

Here we used a compound notation for the differential measure of the p-type flux-tube excitation along with the propagating phase encoded by its energy $E_{\mathbf{p}}$ and momentum $p_{\mathbf{p}}$,

$$d\mu_{\mathbf{p}}(v) = \frac{dv}{2\pi} \mu_{\mathbf{p}}(v) e^{-\tau[E_{\mathbf{p}}(v)-1]+i\sigma p_{\mathbf{p}}(v)} \quad (11)$$

For brevity, we select $\alpha = 4$ component of the \bar{Q}_α^A generator. Its action can be easily evaluated on the twist-one hexagon to read

$$\bar{Q}_4^A e^{-\tau} \mathcal{W}_{6[1](2)} = \chi_4^A e^{-\tau} \int_{\mathbb{R}} d\mu_{\mathbf{g}}(v) \frac{1}{2} (E_{\mathbf{g}}(v) + ip_{\mathbf{g}}(v)) + \dots, \quad (12)$$

where ellipses stand for cyclic contributions accompanied by other Grassmann variables. Expanding the measure, $\mu_{\mathbf{p}} = g^2 \mu_{\mathbf{p}}^{(1)} + g^4 \mu_{\mathbf{p}}^{(2)} + \dots$, the energy and momentum, $E_{\mathbf{p}} = 1 + g^2 E_{\mathbf{p}}^{(1)} + \dots$ and $p_{\mathbf{p}} = 2u + g^2 p_{\mathbf{p}}^{(1)} + \dots$ in perturbative series, we can shift the integration contour in the lower half of the complex rapidity plane, $v \rightarrow v - \frac{i}{2}$ and rewrite the result in the form

$$\begin{aligned} \bar{Q}_4^A e^{-\tau} \mathcal{W}_{6[1](2)} = & -\chi_4^A e^{-\tau} \int_{\mathbb{R}+i0} \frac{dv}{2\pi} e^{2iv\sigma} \left\{ g^2 e^{\sigma} \mu_{\mathbf{F}}^{(1)}(v) \right. \\ & + g^4 \left[e^{\sigma} \left(\mu_{\mathbf{F}}^{(2)}(v) + (i\sigma p_{\mathbf{F}}^{(1)}(v) - \tau E_{\mathbf{F}}^{(1)}(v)) \mu_{\mathbf{F}}^{(1)}(v) \right) - (2\tau + 2\sigma - ip_{\mathbf{g}}^{(1)}(v)) \mu_{\mathbf{g}}^{(1)}(v) \right] \\ & \left. + O(g^6) \right\} + \dots, \end{aligned} \quad (13)$$

at the lowest two orders of perturbation theory. To arrive at this expression we used the following results. First, it is immediate to demonstrate that⁴

$$E_{\mathbf{g}}(v - \frac{i}{2}) = E_{\mathbf{F}}(v) - ip_{\mathbf{f}}(v - i), \quad p_{\mathbf{g}}(v - \frac{i}{2}) = p_{\mathbf{F}}(v) - iE_{\mathbf{f}}(v - i), \quad (14)$$

³ Here and below, we accept a notation that the subscripts in $\mathcal{W}_{N(t_1, \dots, t_{3N-5})[h_1, \dots, h_{3N-5}]}$ stand for the numbers of cusps in the superloop N , with twists t_1, \dots of excitations propagating on sequential intermediate squares and their corresponding total double helicities h_1, \dots .

⁴Cf. these to the relations $E_{\mathbf{F}}(v) - E_{\mathbf{h}}(v - \frac{i}{2}) = ip_{\mathbf{f}}(v)$ and $p_{\mathbf{F}}(v) - p_{\mathbf{h}}(v - \frac{i}{2}) = iE_{\mathbf{f}}(v)$ found in Ref. [13].

by confirming these identities order-by-order in 't Hooft coupling. For the measures, we have in the lowest few orders

$$\begin{aligned} (i-v)\mu_g^{(1)}(v-\frac{i}{2}) &= i\mu_F^{(1)}(v), \\ (i-v)\mu_g^{(2)}(v-\frac{i}{2}) &= i\mu_F^{(2)}(v) - \frac{i}{2}E_g^{(1)}(v-\frac{i}{2})\mu_g^{(1)}(v-\frac{i}{2}) + \frac{\pi(1+2iv)}{v^2(v-i)^2\sinh(\pi v)} \dots \end{aligned}$$

A naked eye inspection of Eq. (13) then immediately suggests that the first line and the first term in the second line emerge from a single-fermion exchange, as anticipated from the Descent Equation. This can be easily verified by computing the σ' integral of the $\chi_1^3\chi_4$ component (18) of the heptagon, see Fig. 1, which is extracted by the $d^{2|3}\mathcal{Z}_1$ measure. It yields to the lowest two orders in g^2

$$\begin{aligned} \int d\sigma' \mathcal{W}_{71,1}^{(4)}(\sigma', \sigma) &= -e^\sigma \int \frac{dv}{2\pi} e^{2iuv} \left\{ g^2 \mu_F^{(1)}(v) \right. \\ &\quad \left. + g^4 \left[\mu_F^{(2)}(v) + (i\sigma p_F^{(1)}(u) - \tau E_F^{(1)}(u) + 2\zeta_2) \mu_F^{(1)}(u) \right] + O(g^6) \right\}, \end{aligned} \quad (15)$$

where σ is associated with the rapidity v and σ' with u , respectively. The ζ_2 term gets cancelled upon multiplication by the cusp anomalous dimension thus providing agreement alluded to above.

However, the second term in the square brackets of Eq. (13) is much more enigmatic. Obviously, there is yet another term that is projected out by the fermionic measure from the heptagon, namely, at leading twist one finds an extra χ_5 term in addition to already addressed χ_4 ,

$$\int d^{2|3}\mathcal{Z}_1 \mathcal{W}_{7,1} = e^{-\tau} \int d\sigma' \left(\chi_4^A \mathcal{W}_{71,1}^{(4)} + \chi_5^A \mathcal{W}_{71,1}^{(5)} \right) + \text{higher twists},$$

So the χ_5 term should be the source of the remaining last term in Eq. (13), which does not admit an obvious OPE interpretation. Thus, one has to understand how it changes as we apply the cyclic permutation to it, i.e., the one that turns $\chi_5 \rightarrow \chi_4$. It appears though that one needs to restore the exact dependence on the cross ratios before moving to a different channel. Is it only possible provided one resums the entire OPE series in this channel? As we will demonstrate below, it is not quite the case but one has to move beyond leading twist in the adjacent channel to induce a leading contribution after the cyclic shift.

4 Fermionic heptagon

As we stated above, we have to unravel the structure of subleading terms in the OPE expansion of fermionic components of the heptagon. Thus we turn to a thorough analysis of $\chi_1^3\chi_4$ and $\chi_1^3\chi_5$ Grassmann structures with emphasis on the lowest twist contribution at the bottom and twist-two on the top. The general form of this expansion takes the form

$$\mathcal{W}_{7,1} = \sum_{j=4,5} \chi_1^3 \chi_j \sum_{n_1, n_2} \sum_{h_1, h_2} e^{-n'\tau' - n\tau} e^{i(h'\phi' + h\phi)/2} \mathcal{W}_{[n', n](h', h)}^{(j)}(\sigma', \sigma; g) + \dots, \quad (16)$$

where the dots stand for irrelevant Grassmann structures and the nomenclature for the labels was explained in the footnote 3.

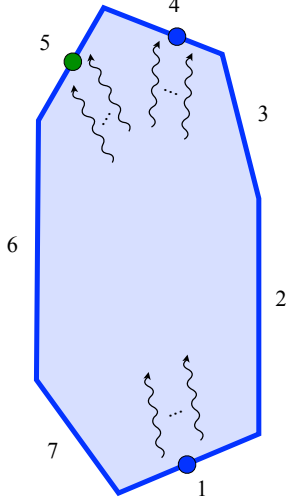


Figure 1: Two OPE channels relevant for the Descent Equation involving heptagon. The two channels are obtained from each other by a mirror reflection with respect to the line going through Z_2 and connecting to the vertex $Z_4 \wedge Z_5$.

4.1 Twist-one: fermion exchange

To start with, we will recall the leading effect from the twist-one fermion propagating in the OPE channels in question [20], i.e., proportional to $e^{-\tau'-\tau} e^{i\phi'/2+i\phi/2}$. Both $\chi_1^3\chi_4$ and $\chi_1^3\chi_5$ Grassmann structures are cumulatively given by

$$\mathcal{W}_{71,1}^{(j)}(\sigma', \sigma) = \int_{\mathbb{C}_{\Psi}^+} d\mu_{\Psi}(u_1) x[u_1] \int_{\mathbb{C}_{\Psi}^{(j)}} d\mu_{\Psi}(v_1) P_{\Psi|\Psi}(-u_1|v_1). \quad (17)$$

They are expressed in terms of the helicity non-flip fermionic pentagon transition $P_{\Psi|\Psi}$ [17] with the measure of the initial-state fermion accompanied by a helicity form factor given by the Zhukowski variable $x[u] = \frac{1}{2}(u + \sqrt{u^2 - (2g)^2})$. Above, the integration contours are shown in Fig. 2. The one for the fermion on the bottom of the heptagon is $\mathbb{C}_{\Psi}^+ = \mathbb{C}_{\mathbb{F}}^+ + \mathbb{C}_{\mathbb{f}}^-$ with $\mathbb{C}_{\mathbb{F}}^+ = \mathbb{R} + i0$ and $\mathbb{C}_{\mathbb{f}}^-$ running a half-circle in the lower semiplane of the complex plane. The top contour depends on the supertwistor which the flux-tube excitation is “attached” to. For the $\chi_1^3\chi_4$ channel it is the same $\mathbb{C}_{\Psi}^{(4)} = \mathbb{C}_{\Psi}^+$, while for $\chi_1^3\chi_5$, it is “flipped” on the Riemann surface with respect to the imaginary axis, i.e., $\mathbb{C}_{\Psi}^{(5)} = \mathbb{C}_{\Psi}^- = \mathbb{C}_{\mathbb{F}}^- + \mathbb{C}_{\mathbb{f}}^+$. It can be explained by the fact that the latter channel is a mirror reflection of the original $\chi_1^3\chi_4$ one, thus in a given tessellation it corresponds to a different collinear limit.

In perturbation theory, since there are no poles in the integrand, only the large fermion contributes to the OPE, yielding

$$\mathcal{W}_{71,1}^{(4,5)}(\sigma', \sigma) = \int_{\mathbb{R}+i0} d\mu_{\mathbb{F}}(u) x[u] \int_{\mathbb{R}\pm i0} d\mu_{\mathbb{F}}(v) P_{\mathbb{F}|\mathbb{F}}(-u|v). \quad (18)$$

Its expansion in 't Hooft coupling can be easily verified to agree with explicit amplitudes by using, for instance, the package of Ref. [29]

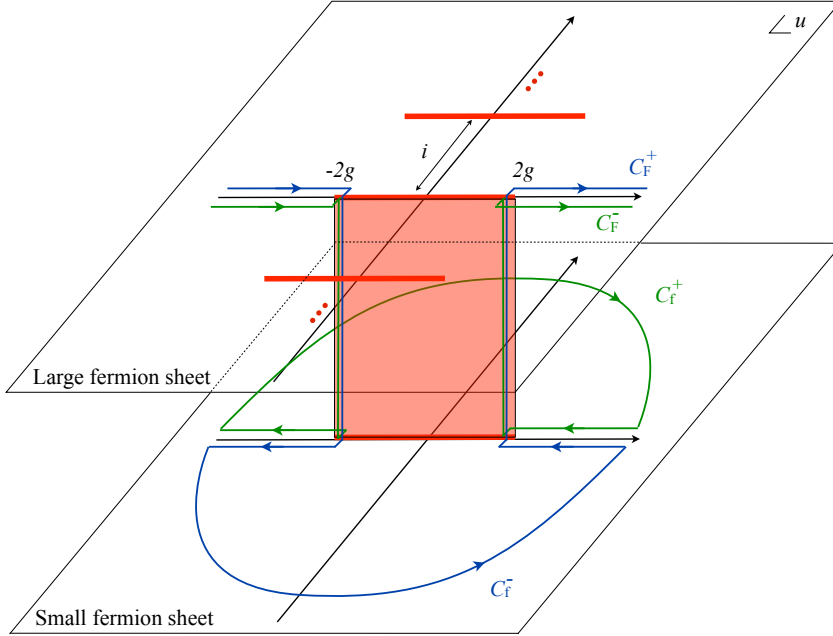


Figure 2: The large and small fermion complex planes are glued together along the square root branch cut on the real axis $[-2g, 2g]$ (shown by the bold red interval) into a two-sheeted Riemann surface. The integration contours for the fermions in the OPE expressions are shown for the χ_4 in blue, $\mathbb{C}_\Psi^+ = \mathbb{C}_F^+ + \mathbb{C}_f^-$, and for χ_5 one in green, $\mathbb{C}_\Psi^- = \mathbb{C}_F^- + \mathbb{C}_f^+$, paths.

4.1.1 Integral of single-particle contribution

The Descent Equation involves an integral over the position σ' . A perturbative analysis to a very high order reveals that the result is given by

$$\Gamma(g) \int d\sigma' \mathcal{W}_{71,1}^{(4)}(\sigma', \sigma) = -2ig^2 \int_{\mathbb{R}+i0} d\mu_\Psi(v_1), \quad (19)$$

where the prefactor of the exact cusp anomalous dimension arises from the integral

$$\int du_1 \mu_\Psi(u_1) e^{-\tau'[E_\Psi(u_1)-1]} x[u_1] \delta(p_\Psi(u_1)) P_{\Psi|\Psi}(-u_1|v_1) = -\frac{2ig^2}{\Gamma(g)}. \quad (20)$$

Superficially the left-hand side depends on the rapidity v_1 , but in reality it is only a function of the 't Hooft coupling. Notice that the dependence on the cross-ratio τ' trivializes in light of the fact that the fermion mass is one at any value of the coupling [30],

$$p_\Psi(u) = 0, \quad E_\Psi(u) = 1. \quad (21)$$

For the $\chi_1^3 \chi_5$ channel, the fermion contour in the final state runs below the real axis. However, due to the Fourier exponent it has to be closed in the upper half plane. As a result of moving the contour just above the real axis, one picks up a pole at $v_1 = 0$ on the real axis. The latter

term induces a divergent contribution when integrated with respect to σ' . Namely, we find that it is coupling independent

$$\operatorname{res}_{v_1=0} P_{\text{F}|F}(-u_1|v_1)\mu_{\text{F}}(v_1)e^{-\tau[E_{\text{F}}(v_1)-1]+i\sigma p_{\text{F}}(v_1)} = -i, \quad (22)$$

such that the two contributions differ by a single-fermion exchange in the NMHV hexagon

$$\mathcal{W}_{71,1}^{(5)}(\sigma', \sigma) = \mathcal{W}_{71,1}^{(4)}(\sigma', \sigma) + \mathcal{W}_{61}(\sigma'), \quad (23)$$

with

$$\mathcal{W}_{61} = -i \int_{\mathbb{R}+i0} d\mu_{\text{F}}(u_1)x[u_1]. \quad (24)$$

It is the last term in the right-hand side that diverges when integrated with respect to σ' . This contribution gets subtracted in the Descent Equation (6) by the last term in its right-hand side.

4.2 Twist-two: fermion-gluon in final state

We now turn to twist-two effects. As exhibited by Eq. (16), at twist-two there is a contribution that enters with the helicity prefactor $e^{3i\phi/2}$. It corresponds to a fermion-gluon pair absorbed by the top portion of the Wilson loop in a given OPE channel. Its all-order expression in coupling constant reads⁵

$$\mathcal{W}_{7[1,2](1,3)}^{(j)} = g \int_{\mathbb{C}_{\Psi}^{\dagger}} d\mu_{\Psi}(u_1) \int_{\mathbb{C}_{\Psi}^{(j)}} d\mu_{\Psi}(v_1) \int_{\mathbb{R}} d\mu_{\text{g}}(v_2) \frac{x[u_1]P_{\Psi|\text{g}}(-u_1|v_2)P_{\Psi|\Psi}(-u_1|v_1)}{\sqrt{x^+[v_2]x^-[v_2]P_{\text{g}|\Psi}(v_2|v_1)P_{\text{g}|\Psi}(-v_2|-v_1)}}, \quad (25)$$

where we used the factorized form of one-to-two particle transition pentagon [20] and fermion-gluon absorption form factor [21]. The helicity form factor is expressed in terms of shifted Zhukowski variables $x^{\pm}[u] \equiv x[u^{\pm}]$ where $u^{\pm} = u \pm \frac{i}{2}$. The bottom fermion resides on the large sheet, while the one on the top can be split in the above formula into the small (f) and large (F) contributions

$$\mathcal{W}_{7[1,2](1,3)}^{(j)} = \mathcal{W}_{7\text{F}|f\text{g}}^{(j)} + \mathcal{W}_{7\text{F}|F\text{g}}^{(j)}. \quad (26)$$

We start with $j = 4$ case first. At lowest two orders in coupling, only the small fermion contributes to the Wilson loop and induces a nontrivial effect that reads

$$\mathcal{W}_{7\text{F}|f\text{g}}^{(4)} = g \int_{\mathbb{R}+i0} d\mu_{\text{F}}(u_1)x[u_1] \int_{\mathbb{R}+i0} d\mu_{\text{gf}}(v_2) \left[\frac{x^-[v_2]}{x^+[v_2]} \right]^{1/2} P_{\text{F}|g}(-u_1|v_2)P_{\text{F}|f}(-u_1|v_2^-), \quad (27)$$

where we introduced the small-fermion-gluon measure [20],

$$\mu_{\text{gf}}(v_2) = \operatorname{res}_{v_1=v_2^-} \frac{g^2 \mu_{\text{f}}(v_1)\mu_{\text{g}}(v_2)}{x[v_1]P_{\text{f}|g}(v_1|v_2)P_{\text{f}|g}(-v_1|-v_2)}. \quad (28)$$

⁵ All pentagon transitions used here and below can be found in Refs. [18, 20, 21].

At $O(g^6)$ and higher, $\mathcal{W}_{7[1,2](1,3)}$ receives an additional term from the large fermion

$$\mathcal{W}_{7\text{F}|Fg}^{(4)} = g \int_{\mathbb{R}+i0} d\mu_F(u_1) \int_{\mathbb{R}+i0} d\mu_F(v_1) \int_{\mathbb{R}+i0} d\mu_g(v_2) \frac{x[u_1]P_{F|g}(-u_1|v_2)P_{F|F}(-u_1|v_1)}{\sqrt{x^+[v_2]x^-[v_2]}P_{g|F}(v_2|v_1)P_{g|F}(-v_2|-v_1)}. \quad (29)$$

Similar analysis can be performed for $j = 5$. The differences in the fermion contour result in differences of various contributions. The small fermion now reads instead

$$\mathcal{W}_{7\text{F}|fg}^{(5)} = g \int_{\mathbb{R}+i0} d\mu_F(u_1)x[u_1] \int_{\mathbb{R}} d\tilde{\mu}_{\text{gf}}(v_2) \left[\frac{x^+[v_2]}{x^-[v_2]} \right]^{1/2} P_{F|g}(-u_1|v_2)P_{F|f}(-u_1|v_2^+), \quad (30)$$

where compared to the previous equation, since the pole $v_2 = v_1^+$ was picked up in the upper half plane of the lower Riemann sheet, the composite measure has changed,

$$\tilde{\mu}_{\text{gf}}(v_2) = \text{res}_{v_1=v_2^+} \frac{g^2 \mu_f(v_1)\mu_g(v_2)}{x[v_1]P_{f|g}(v_1|v_2)P_{f|g}(-v_1|-v_2)}, \quad (31)$$

as well as the square root prefactor was flipped. As above, at order g^6 and beyond, the Wilson loop gets a new term from the large fermion

$$\mathcal{W}_{7\text{F}|Fg}^{(5)} = g \int_{\mathbb{R}+i0} d\mu_F(u_1) \int_{\mathbb{R}-i0} d\mu_F(v_1) \int_{\mathbb{R}+i0} d\mu_g(v_2) \frac{x[u_1]P_{F|g}(-u_1|v_2)P_{F|F}(-u_1|v_1)}{\sqrt{x^+[v_2]x^-[v_2]}P_{g|F}(v_2|v_1)P_{g|F}(-v_2|-v_1)}, \quad (32)$$

which differs from χ_4 by the position of the contour in the large fermion rapidity complex plane. The correctness of these expression can be verified by comparing them in the perturbative expansion with the results of Ref. [29]. It would be important to extend it to higher orders, especially in a fully analytic manner relying on the methods of Ref. [31], using the heptagon bootstrap program [32, 33, 34, 35] that generalizes earlier results on the hexagon [36, 37].

4.2.1 Integral of gluon-fermion contributions

The calculation of the σ' integrals of contributions introduced in the previous section follows the same route as for single fermion in Section 4.1.1, but now we have to evaluate the rapidity integral involving two pentagons. For the $j = 4$ contribution, this can be successfully accomplished order by order in perturbation theory and then resummed back into an exact function of the 't Hooft coupling constant. For the integral involving the small fermion, we find accordingly

$$\int du_1 \mu_F(u_1) e^{-\tau'[E_F(u_1)-1]} x[u_1] \delta(p_F(u_1)) P_{F|f}(-u_1|v_2^-) P_{F|g}(-u_1|v_2) = -\frac{2ig^3}{\Gamma(g)} \frac{1}{\sqrt{x^+[v_2]x^-[v_2]}}. \quad (33)$$

For the one with the large fermion, the expression for the right-hand side looks identical

$$\int du_1 \mu_F(u_1) e^{-\tau'[E_F(u_1)-1]} x[u_1] \delta(p_F(u_1)) P_{F|F}(-u_1|v_1) P_{F|g}(-u_1|v_2) = -\frac{2ig^3}{\Gamma(g)} \frac{1}{\sqrt{x^+[v_2]x^-[v_2]}}. \quad (34)$$

However, a simple counting of the powers of 't Hooft coupling for the large fermion demonstrates that its contribution is postponed one order higher than the integrand itself since the leading term in its expansion vanishes after the u_1 integration. Thus, the large fermion appears accompanied by a gluon starting only from three loops in the Descent Equation.

For $j = 5$, in complete analogy with the single fermion, the σ' integral turns out to be divergent. So it requires a subtraction. To make it as transparent as possible, let us calculate the difference between the χ_5 and χ_4 contributions first. A careful all-order perturbative analysis demonstrates that the latter can be expressed in terms of the following expression

$$\mathcal{W}_{7[1,2](1,3)}^{(5)} - \mathcal{W}_{7[1,2](1,3)}^{(4)} = \Delta\mathcal{W}_{7[1,2](1,3)} \quad (35)$$

with

$$\Delta\mathcal{W}_{7[1,2](1,3)} \equiv \frac{1}{g} \int_{\mathbb{R}+i0} d\mu_{\text{F}}(u_1) \int_{\mathbb{R}+i0} d\mu_{\text{g}}(v_2) x[u_1] P_{\text{F|g}}(-u_1|v_2) \sqrt{x^-[v_2]x^+[v_2]}. \quad (36)$$

It is important to emphasize that, starting from three-loop order, only the total sum of small and large fermion contributions becomes u_1 independent as shown by the factor accompanying $x \mu_{\text{F}} P_{\text{F|g}}$ in the integrand of the above equation!

To proceed further, we form the NMHV ratio functions,

$$\mathcal{P}_{7[1,2](1,3)}^{(j)}(\sigma', \sigma) = \mathcal{W}_{7[1,2](1,3)}^{(j)}(\sigma', \sigma) - \mathcal{W}_{71,1}^{(j)}(\sigma', \sigma) \mathcal{W}_{6[1](2)}(\sigma), \quad (37)$$

with the gluon flux-tube excitation propagating on the bosonic hexagon $\mathcal{W}_{6[1](2)}$, see Eq. (10). Substituting Eq. (23) into above (35), we find

$$\mathcal{P}_{7[1,2](1,3)}^{(5)}(\sigma', \sigma) = \mathcal{P}_{7[1,2](1,3)}^{(4)}(\sigma', \sigma) + [\Delta\mathcal{W}_{7[1,2](1,3)} - \mathcal{W}_{61}(\sigma_1) \mathcal{W}_{6[1](2)}(\sigma)]. \quad (38)$$

The integral of the regularized expression is finite and can be cast in a concise form,

$$\begin{aligned} \int d\sigma' [\Delta\mathcal{W}_{7[1,2](1,3)}(\sigma', \sigma) - \mathcal{W}_{61}(\sigma') \mathcal{W}_{6[1](2)}(\sigma)] \\ = \frac{ig^2}{\Gamma(g)} \int_{\mathbb{R}+i0} d\mu_{\text{g}}(v_2) \left[x^-[v_2] - \frac{g^2}{x^+[v_2]} - \frac{i}{2} (E_{\text{g}}(v_2) + ip_{\text{g}}(v_2)) \right]. \end{aligned} \quad (39)$$

This concludes our discussion of integrals involving fermion-gluon pairs in the OPE of the heptagon.

4.3 Twist-two: antifermion-scalar in final state

Finally, we address the $\mathcal{W}_{7[1,2](1,-1)}^{(j)}$. A simple counting of quantum numbers immediately suggests that there are two additive contributions, one from the hole-antifermion and another from anti-gluon-fermion pair,

$$\mathcal{W}_{7[1,2](1,-1)}^{(j)} = \mathcal{W}_{7\Psi|\bar{\Psi}_{\text{h}}}^{(j)} + \mathcal{W}_{7\Psi|\Psi_{\bar{\text{g}}}}^{(j)}. \quad (40)$$

These admit a representation in terms of pentagons as follows,

$$\mathcal{W}_{7\Psi|\bar{\Psi}_{\text{h}}}^{(j)} = \frac{2}{g^3} \int_{\mathbb{C}_{\Psi}} d\mu_{\Psi}(u_1) \quad (41)$$

$$\begin{aligned}
& \times \int_{\mathbb{C}_{\Psi}^{(j)}} d\mu_{\Psi}(v_1) \int_{\mathbb{R}} d\mu_h(v_2) \frac{x^{3/2}[u_1]x[v_1]P_{\Psi|\bar{\Psi}}(-u_1|v_1)P_{\Psi|h}(-u_1|v_2)}{(v_1 - v_2 - \frac{i}{2})(v_1 - v_2 + \frac{3i}{2})P_{\Psi|h}(v_1|v_2)P_{\Psi|h}(-v_1| - v_2)}, \\
\mathcal{W}_{7F|F\bar{g}}^{(j)} &= g \int_{\mathbb{C}_{\Psi}} d\mu_F(u_1) \\
& \times \int_{\mathbb{C}_{\Psi}^{(j)}} d\mu_F(v_1) \int_{\mathbb{R}+i0} d\mu_g(v_2) \frac{x[u_1]\sqrt{x^+[v_2]x^-[v_2]}P_{\Psi|\Psi}(-u_1|v_1)P_{\Psi|\bar{g}}(-u_1|v_2)}{(v_1 - v_2 - \frac{i}{2})x[v_1]P_{\Psi|\bar{g}}(v_1|v_2)P_{\Psi|\bar{g}}(-v_1| - v_2)}.
\end{aligned} \tag{42}$$

Having these generic expressions, we can rewrite them in specific OPE channels accounting for the difference in the fermionic contours. For $j = 4$ channel, decomposing the fermion into small and large contributions, we obtain

$$\mathcal{W}_{7[1,2](1,-1)}^{(4)} = \mathcal{W}_{7F|\bar{f}h}^{(4)} + \mathcal{W}_{7F|\bar{F}h}^{(4)} + \mathcal{W}_{7F|F\bar{g}}^{(5)}, \tag{43}$$

The first term in the right-hand side starts at order g^2 and induces a tree-level term in the amplitude. The large antifermion–hole sets in an order higher, i.e., $O(g^4)$, while $\mathcal{W}_{7[1,2](1,-1)}^{(4)}$ starts receiving contributions from large-fermion–antigluon pair from two loops. They read individually,

$$\mathcal{W}_{7F|\bar{f}h}^{(4)} = g \int_{\mathbb{R}+i0} d\mu_F(u_1) \int_{\mathbb{R}} d\mu_h(v_2) \mu_f(v_2 - \frac{3i}{2}) \frac{x^{3/2}[u_1]P_{F|\bar{f}}(-u_1|v_2 - \frac{3i}{2})P_{F|h}(-u_1|v_2)}{x[v_2 - \frac{3i}{2}]P_{f|h}(v_2 - \frac{3i}{2}|v_2)P_{f|h}(-v_2 + \frac{3i}{2}| - v_2)}, \tag{44}$$

$$\begin{aligned}
\mathcal{W}_{7F|\bar{F}h}^{(4)} &= \frac{2}{g^3} \int_{\mathbb{R}+i0} d\mu_F(u_1) \\
& \times \int_{\mathbb{R}+i0} d\mu_F(v_1) \int_{\mathbb{R}} d\mu_h(v_2) \frac{x^{3/2}[u_1]x[v_1]P_{F|\bar{F}}(-u_1|v_1)P_{F|h}(-u_1|v_2)}{(v_1 - v_2 - \frac{i}{2})(v_1 - v_2 + \frac{3i}{2})P_{F|h}(v_1|v_2)P_{F|h}(-v_1| - v_2)},
\end{aligned} \tag{45}$$

$$\begin{aligned}
\mathcal{W}_{7F|F\bar{g}}^{(4)} &= g \int_{\mathbb{R}+i0} d\mu_F(u_1) \\
& \times \int_{\mathbb{R}+i0} d\mu_F(v_1) \int_{\mathbb{R}+i0} d\mu_g(v_2) \frac{x[u_1]\sqrt{x^+[v_2]x^-[v_2]}P_{F|F}(-u_1|v_1)P_{F|\bar{g}}(-u_1|v_2)}{(v_1 - v_2 - \frac{i}{2})x[v_1]P_{F|\bar{g}}(v_1|v_2)P_{F|\bar{g}}(-v_1| - v_2)}.
\end{aligned} \tag{46}$$

For $\chi_1^3\chi_5$ channel, all one has to do is to use the corresponding fermion contour. Then one immediately realizes that compared to the previously studied sector, there will be an additional contribution from the small-fermion–antigluon in Eq. (42) due to the location of the simple pole above the real axis where we close our integration contour. Then we have

$$\mathcal{W}_{7[1,2](1,-1)}^{(5)} = \mathcal{W}_{7F|\bar{f}h}^{(5)} + \mathcal{W}_{7F|\bar{F}h}^{(5)} + \mathcal{W}_{7F|f\bar{g}}^{(5)} + \mathcal{W}_{7F|F\bar{g}}^{(5)}. \tag{47}$$

To the lowest two orders of perturbation theory only small fermions contribute to the right-hand side as we now explain. Namely, closing the integration contour in the upper half plane in $\mathcal{W}_{\Psi|\bar{\Psi}h}$ yields the result $\mathcal{W}_{F|\bar{f}h}^{(5)}$

$$\mathcal{W}_{7F|\bar{f}h}^{(5)} = g \int_{\mathbb{R}+i0} d\mu_F(u_1) \int_{\mathbb{R}} d\mu_h(v_2) \mu_f(v_2^+) \frac{x^{3/2}[u_1]P_{F|\bar{f}}(-u_1|v_2^+)P_{F|h}(-u_1|v_2)}{x^+[v_2]P_{f|h}(v_2^+|v_2)P_{f|h}(-v_2^+| - v_2)}. \tag{48}$$

The large-fermion is determined by the integrand of Eq. (45) with the v_2 integral running just below the real axis, $\mathbb{R} - i0$. This contribution vanishes at $O(g^4)$. At this order the small fermion

in the pair with antighuon

$$\mathcal{W}_{7\text{F}|\text{f}\bar{\text{g}}}^{(5)} = \frac{1}{g} \int_{\mathbb{R}+i0} d\mu_{\text{F}}(u_1) x[u_1] \int_{\mathbb{R}} d\mu_{\text{g}}(v_2) \mu_{\text{f}}(v_2^+) x^+[v_2] \sqrt{x^+[v_2] x^-[v_2]} \frac{P_{\text{F}|\text{f}}(-u_1|v_2^+) P_{\text{F}|\bar{\text{g}}}(-u_1|v_2)}{P_{\text{f}|\bar{\text{g}}}(v_2^+|v_2) P_{\text{f}|\bar{\text{g}}}(-v_2^+|-v_2)} \quad (49)$$

starts at one loop, postponing the effect of the large fermion to two loops. The latter is determined by the same equation as in (46), where one has to shift the integration contour with respect to v_2 in the lower half-plane.

Expansion in 't Hooft coupling allows us to confirm these predictions at lowest two orders with explicit amplitudes [29].

4.3.1 Integral of antifermion-hole and fermion-antighuon contributions

To uncover contributions of the above twist-two effects to the Descent Equation, we have to finally evaluate the σ' integrals. Again we start with the convergent $j = 4$ operator channel. To this end, we need the following set of rapidity integrals involving the small antifermion and the hole,

$$\int du_1 \mu_{\text{F}}(u_1) e^{-\tau'[E_{\text{F}}(u_1)-1]} x[u_1] \delta(p_{\text{F}}(u_1)) P_{\text{F}|\bar{\text{f}}}(-u_1|v_2 - \frac{3i}{2}) P_{\text{F}|\text{h}}(-u_1|v_2) = \frac{2g^3}{\Gamma(g)}, \quad (50)$$

the large antifermion and the hole

$$\int du_1 \mu_{\text{F}}(u_1) e^{-\tau'[E_{\text{F}}(u_1)-1]} x[u_1] \delta(p_{\text{F}}(u_1)) P_{\text{F}|\bar{\text{F}}}(-u_1|v_1) P_{\text{F}|\text{h}}(-u_1|v_2) = \frac{2g^3}{\Gamma(g)}, \quad (51)$$

and last but not least, the large fermion and antighuon

$$\int du_1 \mu_{\text{F}}(u_1) e^{-\tau'[E_{\text{F}}(u_1)-1]} x[u_1] \delta(p_{\text{F}}(u_1)) P_{\text{F}|\text{F}}(-u_1|v_1) P_{\text{F}|\bar{\text{g}}}(-u_1|v_2) = -\frac{2g}{\Gamma(g)} \sqrt{x^+[v_2] x^-[v_2]}. \quad (52)$$

Now we move to the $j = 5$ case. First for antifermion-hole contribution $\mathcal{W}_{7\Psi|\bar{\Psi}\text{h}}^{(5)}$, we find that the integral involving the small antifermion is identical to Eq. (50). In fact, these two are particular cases of a more general formula for a generic value of v_1 in $P_{\text{F}|\bar{\text{f}}}(-u_1|v_1)$. Next, for the large fermion we can use Eq. (51) in spite of the fact that the integration contour for the outgoing fermion lies below the real axis. The reason for this is that while crossing the real axis one acquires a pole along the way, this term is not singular for $u_1 = 0$. Finally, we turn to the antighuon-fermion final state, $\mathcal{W}_{7\Psi|\Psi\bar{\text{g}}}^{(5)}$. In this case, the σ' integral is not convergent, so one has to form the ratio function and thus subtract a factorized contribution,

$$\mathcal{P}_{7[1,2](1,-1)}^{(5)}(\sigma', \sigma) = \mathcal{W}_{7[1,2](1,-1)}^{(5)}(\sigma', \sigma) - \mathcal{W}_{71,1}^{(5)}(\sigma', \sigma) \mathcal{W}_{6[1](2)}(\sigma). \quad (53)$$

Substituting (23), we can split the result into two terms,

$$\begin{aligned} \mathcal{W}_{7\Psi|\Psi\bar{\text{g}}}^{(5)}(\sigma', \sigma) - \mathcal{W}_{71,1}^{(5)}(\sigma', \sigma) \mathcal{W}_{6[1](2)}(\sigma) \\ = \mathcal{W}_{7\Psi|\Psi\bar{\text{g}}}^{(4)}(\sigma', \sigma) - \mathcal{W}_{71,1}^{(4)}(\sigma', \sigma) \mathcal{W}_{6[1](2)}(\sigma) \end{aligned} \quad (54)$$

$$+ \left[\Delta \mathcal{W}_{7\Psi|\Psi\bar{g}}^{(5)}(\sigma', \sigma) - \mathcal{W}_{61}(\sigma') \mathcal{W}_{6[1](2)}(\sigma) \right],$$

with the first two terms in its right-hand side addressed in previous sections. The integral of the square bracket can be expressed in a concise form

$$\begin{aligned} \int_0^\infty d\sigma' \left[\Delta \mathcal{W}_{7\Psi|\Psi\bar{g}}^{(5)}(\sigma', \sigma) - \mathcal{W}_{61}(\sigma') \mathcal{W}_{6[1](2)}(\sigma) \right] \\ = \frac{ig^2}{\Gamma(g)} \int d\mu_g(v_2) \left[-x^-[v_2] + \frac{g^2}{x^+[v_2]} - \frac{i}{2} (E_g(v_2) + ip_g(v_2)) \right]. \end{aligned} \quad (55)$$

One can combine all of the above ingredients together and substitute them into the Descent Equation. We will not give the cumulative formula here to save space. It is obvious from the representation of these results, that the overall power of the inverse cusp anomalous dimension cancels against the one in the right-hand side of Eq. (6). Thus, this proves the all-order form of the Descent Equation provided that we can establish an agreement between OPE series on both of its sides. This is what we will accomplish next getting some inspiration from perturbation theory.

4.4 Cyclic permutation at one loop

Having analyzed all twist-two flux-tube excitations in the two channels of interest, we have to find a way to cyclically shift $j = 5$ channel down to $j = 4$. Since we currently lack a dynamical understanding of this mechanism from the point of view of underlying flux-tube dynamics, we will choose a more pragmatic route. As a guidance, we will start with an exact expression for the one-loop heptagon and work out the Descent Equation for it. According to Eq. (6), the action of the \bar{Q} generator on the two-loop bosonic hexagon yields [26]

$$\begin{aligned} \bar{Q}_\alpha^A \mathcal{W}_{6,0} = \bar{Q}_\alpha^A \ln \frac{\langle 6724 \rangle}{\langle 6723 \rangle} \int_0^\infty dt I^{(4)}(t|u_1, u_2, u_3, v) \\ + \bar{Q}_\alpha^A \ln \frac{\langle 6725 \rangle}{\langle 6723 \rangle} \int_0^\infty dt I^{(5)}(t|u_1, u_2, u_3, v) + \text{cyclic}, \end{aligned} \quad (56)$$

where the right-hand side receives contributions from the $\chi_1^3 \chi_4$ and $\chi_1^3 \chi_5$ structures, in the first and second term, respectively, and corresponds in the OPE language to a single fermion at the bottom of the heptagon and all twists absorbed at the top. The collinear expansion on the top of the heptagon admits a systematic classification within the pentagon framework, namely, we immediately find

$$e^{2\sigma'} I_4(e^{2\sigma'} | u_1, u_2, u_3, v) = -e^{-\tau} \mathcal{P}_{71,1}^{(4)}(\sigma', \sigma, \tau' = 0, \tau) \quad (57)$$

$$- e^{-2\tau} \left(e^{i\phi} \mathcal{P}_{7[1,2](1,3)}^{(4)} + e^{-i\phi} \mathcal{P}_{7[1,2](1,-1)}^{(4)} \right) (\sigma', \sigma, \tau' = 0, \tau) + O(e^{-3\tau}),$$

$$e^{2\sigma'} I_5(e^{2\sigma'} | u_1, u_2, u_3, v) = -e^{-\tau} \mathcal{P}_{71,1}^{(5)}(\sigma', \sigma, \tau' = 0, \tau) \quad (58)$$

$$- e^{-2\tau} \left(e^{i\phi} \mathcal{P}_{7[1,2](1,3)}^{(5)} + e^{-i\phi} \mathcal{P}_{7[1,2](1,-1)}^{(5)} \right) (\sigma', \sigma, \tau' = 0, \tau) + O(e^{-3\tau}),$$

where the remaining dependence of the ratio functions on the τ and τ' is polynomial due to higher order corrections to eigen-energies of flux-tube excitations. Above, we set τ' to zero everywhere since these contributions vanish after σ' integration owing to the Goldstone theorem [30].

Finally, we have to move the χ_5 contribution to the χ_4 channel. This is achieved by a cyclic shift of twistors that results in a change of cross ratios as shown in Eqs. (65). We will use the exact expression for I_5 [26],

$$\begin{aligned}
I_5(t|u_1, u_2, u_3, v) = & -\frac{u_3}{t(u_3+t)} \left[-\ln(1+t) \ln \frac{1+t}{t} - \ln \frac{u_3(1+t)}{u_3+t} \ln \frac{u_2(u_3+t)}{t} \right. \\
& + \text{Li}_2(1-u_2) + \text{Li}_2(1-u_3) - \text{Li}_2\left(\frac{1-u_3}{1+t}\right) + \text{Li}_2\left(1-\frac{u_2}{1+t}\right) \\
& + \frac{1}{t(u_3+t)} \left[\ln \frac{u_3(u_3+t)}{u_3+t} \ln \frac{u_3+t}{t} + \text{Li}_2(1-u_1) - \text{Li}_2\left(1-\frac{u_1 t_1}{u_3+t}\right) \right] \\
& \left. + \frac{v-u_3}{1+t} \left[\ln \frac{u_2}{1+t} \ln \frac{u_1 t}{u_3+t} + \text{Li}_2\left(1-\frac{u_2}{1+t}\right) + \text{Li}_2\left(1-\frac{u_1 t}{u_3+t}\right) - \zeta_2 \right]. \right. \tag{59}
\end{aligned}$$

Then the transition to the cyclic channel, is achieved by replacing the conformal cross ratios $u \rightarrow \tilde{u}$ summarized in Appendix A. Expanding the result at $\tau \rightarrow \infty$, we deduce the following expression after integration with respect to σ'

$$\begin{aligned}
\int_{-\infty}^{\infty} d\sigma' e^{2\sigma'} I_5(e^{2\sigma'}|\tilde{u}_1, \tilde{u}_2, \tilde{u}_3, \tilde{v}) = & 0 - e^{-\tau} \int_{-\infty}^{\infty} d\sigma' \left[i \left(\mathcal{P}_{7[1,2](1,3)}^{(5)} - \mathcal{P}_{7[1,2](1,-1)}^{(5)} \right) \sin \phi \right. \\
& \left. + \left(\mathcal{P}_{7[1,2](1,-1)}^{(4)} + \mathcal{P}_{7[1,2](1,3)}^{(4)} - \mathcal{P}_{7[1,2](1,3)}^{(5)} - \mathcal{P}_{7[1,2](1,-1)}^{(5)} + e^\sigma \mathcal{P}_{71,1}^{(4)} \right) \cos \phi \right] + O(e^{-2\tau}). \tag{60}
\end{aligned}$$

Here the leading-twist effect vanishes upon integration! The subleading terms are expressed in terms of OPE exchanges worked out above for the χ_4 and χ_5 Grassmann components. The parity-even term here defines the leading contribution to the χ_4 -channel of the Descent Equation after the cyclic shift. This is the effect of twist enhancement we alluded to in the Introduction. This expression can be cast in a very concise form at this order in the coupling, namely,

$$\begin{aligned}
2 \int_{-\infty}^{\infty} d\sigma' \left(\mathcal{P}_{7[1,2](1,-1)}^{(4)} + \mathcal{P}_{7[1,2](1,3)}^{(4)} - \mathcal{P}_{7[1,2](1,3)}^{(5)} - \mathcal{P}_{7[1,2](1,-1)}^{(5)} + e^\sigma \mathcal{P}_{71,1}^{(4)} \right) \tag{61} \\
= -g^4 \int_{\mathbb{R}+i0} \frac{dv_1}{2\pi} e^{2iv_1\sigma} \mu_g^{(1)}(v_1) (2\tau + 2\sigma - ip_g^{(1)}(v_1)) + O(g^6).
\end{aligned}$$

As we can see, the $O(g^4)$ contribution is in agreement with the last term in Eq. (13). It is important to realize, however, that at one-loop the left-hand side is not unique. Namely, there is a relation between $\mathcal{W}_{7[1,2](1,-1)}^{(4)}$ and $\mathcal{W}_{7[1,2](1,3)}^{(4)}$ components of the superloop,

$$\mathcal{W}_{7[1,2](1,-1)}^{(4)} = \mathcal{W}_{7[1,2](1,3)}^{(4)} + e^\sigma \mathcal{W}_{71,1}^{(4)} + O(g^6), \tag{62}$$

which is valid to order g^4 only and thus implies that one can replace $\mathcal{P}_{7[1,2](1,-1)}^{(4)} + \mathcal{P}_{7[1,2](1,3)}^{(4)} + e^\sigma \mathcal{P}_{71,1}^{(4)} \rightarrow 2\mathcal{P}_{7[1,2](1,-1)}^{(4)}$ in the above equation. Taken at its face value, this relation yields an incorrect OPE representation for the $\mathcal{P}_{7[1,2](1,-1)}^{(4)}$ since in the lowest two orders of perturbation theory the left-hand side can be cast in the form (48). Obviously, the pole at $v_2 = v_1^+$ is not at the right side of the real axis to be naturally accommodated into OPE. There is an immediate problem that one needs to reconcile, namely, how the two results, Eq. (48) and (43) can be compatible. The first one has only small fermion contribution while the latter one has both,

large and small. It turns out that if one ignores the proper choice of the contour and uses \mathbb{C}_ψ^- instead of \mathbb{C}_ψ^+ , then \mathbb{C}_f^+ is closed in the upper half plane and one picks up a pole at $v_2 = v_1^+$ and gets the result given in Eq. (48). At the same time, as we already mentioned before, the genuine two-particle twist-two contribution (that sets in at order g^4) vanishes, so one is left with small-fermion–hole pair alone as found in the relation (62).

Therefore, to put the result (61) on a firmer foundation, we compared the left- and right-hand sides of the Descent Equation at $O(g^6)$, when all two-particle excitations contribute to the OPE. As a result, we confirmed the agreement, i.e., the equality of Eq. (12) to the sum of Eq. (19) and (61) multiplied by the factor of the cusp anomalous dimension. This is the main result of this paper.

5 Conclusions

In this work, we analyzed the Descent Equation within the OPE. We demonstrated that the factor of the cusp anomalous dimensions naturally arises in its right-hand side from the pentagon framework confirming in this manner the all loop structure of the Descent Equation. We have established a phenomenon of twist enhancement as one passes from direct to a cyclic channel. Namely, the leading effect emerges from the subleading contribution in the adjacent channel. Added up with the twist one excitations in the direct channel, it proves the consistency of the OPE expansion with the \bar{Q} -equation. It would be interesting to extend this consideration to event higher twists and other nonMHV polygons.

It is very important to understand the twist enhancement from the underlying flux-tube picture. A handwaving argument along the lines, that one can move the fermionic excitation on the top of the polygon from one site to another making use of a “mirror” transformation for the fermion which increases its twist and promotes it to a string of two excitation separated in the rapidity space [17], is too vague and imprecise. Moreover, from the point of view of explicit calculations, this could only account for some of the contributions.

As a next step it is interesting to focus on the structure of the equation at strong coupling⁶. Contrary to weak coupling, as $g \rightarrow \infty$ the large fermion decouples since its energy and momentum scale with g , while the small fermion’s mass remains unrenormalized. A quick look at the left-hand side of the Descent Equation demonstrates that the structure of propagating exponent is very suggestive if one shifts the integration contour and uses the all-order relations (14). However to correctly reproduce the prefactor, one has to understand how the cyclic channel gets added to the total result. A rather subtle issue to be addressed is about composite states involving a fermion an arbitrary number of massless (at strong coupling) holes that contribute on equal footing with a single small fermion, see, e.g., Ref. [39]. These questions will be addressed in a future publication.

Acknowledgments

We would like to thank Jacob Bourjaily for very instructive correspondence and the organizers of the “Flux-tube Workshop” for hospitality at Perimeter Institute at the final stages of this work. This research was supported by the U.S. National Science Foundation under the grants PHY-1068286 and PHY-1403891.

⁶See recent work on resummation of the OPE series and its agreement with TBA [38]

A Parametrization of polygons

Making use of the projective invariance of momentum twistors, we will use the following rescaled version of the later for the hexagon

$$\begin{aligned}
Z_1^{(6)} &= (e^{-\tau+2\sigma}, 0, e^{\sigma+i\phi}, e^{-2\tau+\sigma+i\phi}), \\
Z_2^{(6)} &= (1, 0, 0, 0), \\
Z_3^{(6)} &= (-1, 0, 0, 1), \\
Z_4^{(6)} &= (0, 1, -1, 1), \\
Z_5^{(6)} &= (0, 1, 0, 0), \\
Z_6^{(6)} &= (0, e^{-\tau}, e^{\sigma+i\phi}, 0),
\end{aligned} \tag{63}$$

and heptagon

$$\begin{aligned}
Z_1^{(7)} &= (e^{-\tau'+2\sigma'}, 0, e^{\sigma'+i\phi'}, e^{-2\tau'+\sigma'+i\phi'}), \\
Z_2^{(7)} &= (1, 0, 0, 0), \\
Z_3^{(7)} &= (-1, 0, 0, 1), \\
Z_4^{(7)} &= (-e^{-\tau}, e^{-\sigma-i\phi}, -e^{-\sigma-i\phi}, e^{-\sigma-i\phi}(1 + e^{-2\tau}) + e^{-\tau}), \\
Z_5^{(7)} &= (0, e^{-\sigma-i\phi} + e^{-\tau-2\sigma}, -e^{-\sigma-i\phi}, e^{-\sigma-i\phi}), \\
Z_6^{(7)} &= (0, 1, 0, 0), \\
Z_7^{(7)} &= (0, e^{-\tau'}, e^{\sigma'+i\phi'}, 0),
\end{aligned} \tag{64}$$

respectively, compared to Refs. [16, 21]. These are very well suited for the collinear expansion within the framework of the Descent Equation, in particular ensuring Eq. (7).

The collinear limit $Z_1 \rightarrow Z_7$ at the bottom of the heptagon leaves just three conformal cross ratios analogous to the one of the hexagon and one non-spacetime cross ratio

$$\begin{aligned}
u_1 &= \frac{(2, 3, 4, 5)(5, 6, 7, 2)}{(2, 3, 5, 6)(4, 5, 7, 2)} \Big|_{\tau' \rightarrow \infty} = \frac{e^{i\phi}}{e^{2\sigma+i\phi} + e^{-\tau+\sigma} + e^{-\tau+\sigma+2i\phi} + e^{i\phi}(1 + e^{-2\tau})}, \\
u_2 &= \frac{(3, 4, 5, 6)(6, 7, 2, 3)}{(3, 4, 6, 7)(2, 3, 5, 6)} \Big|_{\tau' \rightarrow \infty} = \frac{e^{-2\tau}}{1 + e^{-2\tau}}, \\
u_3 &= \frac{(4, 5, 6, 7)(7, 2, 3, 4)}{(4, 5, 7, 2)(3, 4, 6, 7)} \Big|_{\tau' \rightarrow \infty} = \frac{e^{2\sigma}}{1 + e^{-2\tau}} u_1, \\
v &= \frac{(6, 7, 3, 5)(7, 2, 3, 4)}{(6, 7, 3, 4)(7, 2, 3, 5)} \Big|_{\tau' \rightarrow \infty} = \frac{e^\sigma}{(1 + e^{-2\tau})(e^\sigma + e^{-\tau+i\phi})}.
\end{aligned}$$

We also introduce cyclically shifted cross ratios $i \rightarrow i + 1$,

$$\begin{aligned}
\tilde{u}_1 &= \frac{(3, 4, 5, 6)(6, 7, 2, 3)}{(3, 4, 6, 7)(5, 6, 2, 3)} \Big|_{\tau' \rightarrow \infty} = u_2, \\
\tilde{u}_2 &= \frac{(4, 5, 6, 7)(7, 2, 3, 4)}{(4, 5, 7, 2)(3, 4, 6, 7)} \Big|_{\tau' \rightarrow \infty} = u_3,
\end{aligned} \tag{65}$$

$$\begin{aligned}\tilde{u}_3 &= \frac{(5, 6, 7, 2)(2, 3, 4, 5)}{(5, 6, 2, 3)(4, 5, 7, 2)} \Big|_{\tau' \rightarrow \infty} = u_1, \\ \tilde{v} &= \frac{(7, 2, 4, 6)(2, 3, 4, 5)}{(7, 2, 4, 5)(2, 3, 4, 6)} \Big|_{\tau' \rightarrow \infty} = (1 + e^{-\tau + \sigma + i\phi} + e^{-2\tau}) u_1.\end{aligned}$$

The latter will be relevant for establishing the form of the cyclic permutation form of the χ_5 contribution to the one-loop heptagon.

References

- [1] L.F. Alday, J.M. Maldacena, “Gluon scattering amplitudes at strong coupling,” *JHEP* **0706** (2007) 064 [arXiv:0705.0303 [hep-th]].
- [2] J.M. Drummond, J. Henn, G.P. Korchemsky, E. Sokatchev, “On planar gluon amplitudes/Wilson loops duality,” *Nucl. Phys. B* **795** (2008) 52 [arXiv:0709.2368 [hep-th]].
- [3] A. Brandhuber, P. Heslop, G. Travaglini, “MHV amplitudes in N=4 super Yang-Mills and Wilson loops,” *Nucl. Phys. B* **794** (2008) 231 [arXiv:0707.1153 [hep-th]].
- [4] S. Caron-Huot, “Notes on the scattering amplitude / Wilson loop duality,” *JHEP* **1107** (2011) 058 [arXiv:1010.1167 [hep-th]].
- [5] L.J. Mason, D. Skinner, “The Complete Planar S-matrix of N=4 SYM as a Wilson Loop in Twistor Space,” *JHEP* **1012** (2010) 018 [arXiv:1009.2225 [hep-th]].
- [6] A.V. Belitsky, G.P. Korchemsky, E. Sokatchev, “Are scattering amplitudes dual to super Wilson loops?,” *Nucl. Phys. B* **855** (2012) 333 [arXiv:1103.3008 [hep-th]].
- [7] L.F. Alday, D. Gaiotto, J. Maldacena, A. Sever, P. Vieira, “An Operator Product Expansion for Polygonal null Wilson Loops,” *JHEP* **1104** (2011) 088 [arXiv:1006.2788 [hep-th]].
- [8] D. Gaiotto, J. Maldacena, A. Sever, P. Vieira, “Pulling the straps of polygons,” *JHEP* **1112** (2011) 011 [arXiv:1102.0062 [hep-th]].
- [9] A.V. Belitsky, “OPE for null Wilson loops and open spin chains,” *Phys. Lett. B* **709** (2012) 280 [arXiv:1110.1063 [hep-th]].
- [10] A. Sever, P. Vieira, T. Wang, “From Polygon Wilson Loops to Spin Chains and Back,” *JHEP* **1212** (2012) 065 [arXiv:1208.0841 [hep-th]].
- [11] B. Basso, A. Sever, P. Vieira, “Spacetime and Flux Tube S-Matrices at Finite Coupling for N=4 Supersymmetric Yang-Mills Theory,” *Phys. Rev. Lett.* **111** (2013) 9, 091602 [arXiv:1303.1396 [hep-th]].
- [12] B. Basso, “Exciting the GKP string at any coupling,” *Nucl. Phys. B* **857** (2012) 254 [arXiv:1010.5237 [hep-th]].
- [13] B. Basso, A.V. Belitsky, “Lüscher formula for GKP string,” *Nucl. Phys. B* **860** (2012) 1 [arXiv:1108.0999 [hep-th]].

- [14] D. Fioravanti, S. Piscaglia, M. Rossi, “On the scattering over the GKP vacuum,” *Phys. Lett. B* **728** (2014) 288 [arXiv:1306.2292 [hep-th]].
- [15] B. Basso, A. Rej, “Bethe ansatz for GKP strings,” *Nucl. Phys. B* **879** (2014) 162 [arXiv:1306.1741 [hep-th]].
- [16] B. Basso, A. Sever, P. Vieira, “Space-time S-matrix and Flux tube S-matrix II. Extracting and Matching Data,” *JHEP* **1401** (2014) 008 [arXiv:1306.2058 [hep-th]].
- [17] B. Basso, A. Sever, P. Vieira, “Space-time S-matrix and Flux-tube S-matrix III. The two-particle contributions,” *JHEP* **1408** (2014) 085 [arXiv:1402.3307 [hep-th]].
- [18] A.V. Belitsky, “Nonsinglet pentagons and NMHV amplitudes,” *Nucl. Phys. B* **896** (2015) 493 [arXiv:1407.2853 [hep-th]].
- [19] B. Basso, A. Sever, P. Vieira, “Space-time S-matrix and Flux-tube S-matrix IV. Gluons and Fusion,” *JHEP* **1409** (2014) 149 [arXiv:1407.1736 [hep-th]].
- [20] A.V. Belitsky, “Fermionic pentagons and NMHV hexagon,” *Nucl. Phys. B* **894** (2015) 108, [arXiv:1410.2534 [hep-th]].
- [21] A.V. Belitsky, “On factorization of multiparticle pentagons,” *Nucl. Phys. B* **897** (2015) 346 [arXiv:1501.06860 [hep-th]].
- [22] B. Basso, J. Caetano, L. Cordova, A. Sever, P. Vieira, “OPE for all Helicity Amplitudes,” arXiv:1412.1132 [hep-th].
- [23] J.M. Drummond, J. Henn, G.P. Korchemsky, E. Sokatchev, “Dual superconformal symmetry of scattering amplitudes in N=4 super-Yang-Mills theory,” *Nucl. Phys. B* **828** (2010) 317 [arXiv:0807.1095 [hep-th]].
- [24] L.J. Mason, D. Skinner, “Dual Superconformal Invariance, Momentum Twistors and Grassmannians,” *JHEP* **0911** (2009) 045 [arXiv:0909.0250 [hep-th]].
- [25] N. Arkani-Hamed, J. Trnka, “The Amplituhedron,” *JHEP* **1410** (2014) 30 [arXiv:1312.2007 [hep-th]]; “Into the Amplituhedron,” *JHEP* **1412** (2014) 182 [arXiv:1312.7878 [hep-th]].
- [26] S. Caron-Huot, S. He, “Jumpstarting the All-Loop S-Matrix of Planar N=4 Super Yang-Mills,” *JHEP* **1207** (2012) 174 [arXiv:1112.1060 [hep-th]].
- [27] M. Bullimore, D. Skinner, “Descent Equations for Superamplitudes,” arXiv:1112.1056 [hep-th].
- [28] A. Hodges, Eliminating spurious poles from gauge-theoretic amplitudes, *JHEP* **1305** (2013) 135 [arXiv:0905.1473 [hep-th]].
- [29] J.L. Bourjaily, S. Caron-Huot, J. Trnka, “Dual-Conformal Regularization of Infrared Loop Divergences and the Chiral Box Expansion,” *JHEP* **1501** (2015) 001 [arXiv:1303.4734 [hep-th]].
- [30] L.F. Alday, J.M. Maldacena, “Comments on operators with large spin,” *JHEP* **0711** (2007) 019 [arXiv:0708.0672 [hep-th]].

- [31] G. Papathanasiou, “Hexagon Wilson Loop OPE and Harmonic Polylogarithms,” JHEP **1311** (2013) 150 [arXiv:1310.5735 [hep-th]].
- [32] J. Golden, M.F. Paulos, M. Spradlin, A. Volovich, “Cluster Polylogarithms for Scattering Amplitudes,” J. Phys. A **47** (2014) 47, 474005 [arXiv:1401.6446 [hep-th]].
- [33] J. Golden, M. Spradlin, “An analytic result for the two-loop seven-point MHV amplitude in $\mathcal{N} = 4$ SYM,” JHEP **1408** (2014) 154 [arXiv:1406.2055 [hep-th]].
- [34] J. Golden, M. Spradlin, “A Cluster Bootstrap for Two-Loop MHV Amplitudes,” JHEP **1502** (2015) 002 [arXiv:1411.3289 [hep-th]].
- [35] J.M. Drummond, G. Papathanasiou, M. Spradlin, “A Symbol of Uniqueness: The Cluster Bootstrap for the 3-Loop MHV Heptagon,” JHEP **1503** (2015) 072 [arXiv:1412.3763 [hep-th]].
- [36] L.J. Dixon, J.M. Drummond, J.M. Henn, “Analytic result for the two-loop six-point NMHV amplitude in N=4 super Yang-Mills theory,” JHEP **1201** (2012) 024 [arXiv:1111.1704 [hep-th]].
- [37] L.J. Dixon, M. von Hippel, “Bootstrapping an NMHV amplitude through three loops,” JHEP **1410** (2014) 65 [arXiv:1408.1505 [hep-th]].
- [38] D. Fioravanti, S. Piscaglia, M. Rossi, “Asymptotic Bethe Ansatz on the GKP vacuum as a defect spin chain: scattering, particles and minimal area Wilson loops,” arXiv:1503.08795 [hep-th].
- [39] B. Basso, A. Sever, P. Vieira, “Collinear Limit of Scattering Amplitudes at Strong Coupling,” Phys. Rev. Lett. **113** (2014) 26, 261604 [arXiv:1405.6350 [hep-th]].